Effect of the Si/B ratio on the magnetic anisotropy distribution of $Fe_{73.5}Si_{22.5-x}B_xCu_1Nb_3$ ($x=7,9,16$) alloys along nanocrystallization

V. Franco, C. F. Conde, and A. Conde[a)]
Departamento de Física de la Materia Condensada, Universidad de Sevilla, Apdo. 1065, 41080 Sevilla, Spain

(Received 20 March 1998; accepted for publication 14 July 1998)

The effect of the Si/B ratio on the magnetic anisotropy distribution of $Fe_{73.5}Si_{22.5-x}B_xCu_1Nb_3$ ($x=7,9,16$) alloys has been studied. The influence of isochronal annealing on the hysteresis loop of the three studied alloys has been analyzed. They present two minima in coercivity: the first one can be ascribed to structural relaxation, and the second one is related to the averaging of the magnetocrystalline anisotropy, as predicted by the random anisotropy model. The relative importance of both minima changes with Si content: the lower the Si content, the more effective the structural relaxation and the less important the second minimum are. The mean value of the magnetic anisotropy distribution presents a similar behavior, evidencing the growing importance of the magnetoelastic anisotropy for the relaxed amorphous samples as the Si content is increased. From the evolution of the magnetic anisotropy distribution along nanocrystallization and the microstructural information obtained from transmission electron microscopy images, the behavior of the coercivity minima with changes in Si content can be ascribed to a different degree in compensation of magnetoelastic anisotropy due to the contributions of different signs coming from the nanocrystals and the amorphous matrix. © *1998 American Institute of Physics.* [S0021-8979(98)04820-8]

I. INTRODUCTION

Since its discovery by Yoshizawa *et al.*,[1] the amorphous ferromagnetic alloy known under the trade name of FINEMET has attracted much scientific interest due to its outstanding soft magnetic properties. This alloy, with a composition of $Fe_{73.5}Si_{13.5}B_9Cu_1Nb_3$, is suitable not only for many technological applications but for performing a considerable amount of fundamental studies in magnetism. Its softest properties are obtained after nanocrystallization, while it is constituted of two phases: an ultrafine grained Fe,Si phase which is embedded in the remaining amorphous matrix.

The role of the Cu and Nb elements in the achievement of this microstructure and its relationship with the magnetic properties has been thoroughly studied.[2,3] Copper, which is nonsoluble in bcc iron, segregates prior to or at the very beginning of nanocrystallization, forming Cu-rich clusters, and the nucleation of Fe,Si grains is thought to be multiplied by clustering. On the other hand, the rejection of Nb at the crystal interfaces hinders grain growth. The effect of the substitution of copper by other elements which are soluble in bcc Fe has also been reported,[4,5] confirming the importance of the nonsolubility of Cu for the achievement of this special microstructure and its characteristic magnetic properties. There has also been some studies devoted to the correlation of the magnetic properties with the change of the Si/B ratio in the alloy,[6–8] or with the Fe/Nb ratio.[9]

Recently, changes in magnetic anisotropy distribution upon heat treatment of a nanocrystalline material have been presented.[10] These results fall out of the capabilities of Herzer's model.[11] In order to explain the magnetic hardening which takes place at the very beginning of nanocrystallization, a generalization of the random anisotropy model has been developed[12] that takes into account the two-phase character of nanocrystalline materials. This model can also account for the evolution of the magnetic anisotropy distribution along the first crystallization stage.

This work is devoted to the first crystallization stage of $Fe_{73.5}Si_{22.5-x}B_xCu_1Nb_3$ ($x=7,9,16$) and to the influence of the Si/B ratio on the magnetic properties of the alloys along nanocrystallization. Although FINEMET-type alloys are usually regarded as magnetically softer after nanocrystallization than in the amorphous state, it can be easily seen that slight changes in composition make this sentence untrue. There has been previous studies of the magnetic properties of these alloys; however, to our knowledge none of them presented either the influence of the changes in composition on the distribution of magnetic anisotropy or its effect on the relative importance of the coercivity minima (before and after nanocrystallization). As magnetic anisotropy is exploited in the design of most magnetic materials of commercial interest, its distribution in the FINEMET-type alloys is worth studying. Also, this study will provide us with valuable information about the alloys themselves along nanocrystallization and will support an explanation of the compositional dependence of the relative importance of the two coercivity minima.

a)Electronic mail: conde@cica.es

II. EXPERIMENT

Amorphous ribbons of alloys with nominal compositions of $Fe_{73.5}Si_{22.5-x}B_xCu_1Nb_3$ ($x=7,9,16$) were prepared by a melt-spinning technique in the Institute of Physics of the Slovak Academy of Sciences in Bratislava.

Specimens for transmission electron microscopy (TEM) studies were prepared by using a twin-jet electrochemical polishing device with a 10% perchloric acid–acetic acid solution. TEM observations were performed on an Hitachi H-800 electron microscope with an accelerating voltage of 200 kV.

Quasistatic M-H hysteresis loops were measured at room temperature by using a computerized loop tracer developed at our laboratory.[13] Samples 10 cm long, 25 μm thick, and 1 cm wide were previously submitted to 1 h isochronal annealing in a halogen-lamp furnace under argon atmosphere.

The magnetic anisotropy distribution can be obtained directly from the magnetization curve.[14] To do that, let us consider a distribution of uniaxial local easy axes with different strength but all directed at right angles with respect to the applied field. The anisotropy field H^K can be defined as the field necessary to saturate a uniaxial particle at right angles to its easy axis and is related to the anisotropy constant K by

$$2K=\mu_0 M_s H^K, \tag{1}$$

where M_s is the saturation magnetization. Thus, a region of such an ensemble of easy axes, characterized by an anisotropy field H^K, under the influence of a field H perpendicular to the easy axes will magnetize in the following way:

$$\begin{aligned} M(H,H^K)&=M_s\times(H/H^K) \quad \text{for } H<H^K,\\ M(H,H^K)&=M_s \quad \text{for } H>H^K. \end{aligned} \tag{2}$$

Let us define $P(H^K)$ as the normalized probability of finding the value H^K for the anisotropy field. By normalization we mean that the total probability of finding an anisotropy value greater than zero is unity

$$\int_0^\infty P(H^K)dH^K=1. \tag{3}$$

Consequently, the macroscopic reduced magnetization ($m=M/M_s$) of the whole ensemble will be

$$\langle m(H)\rangle=m_r+\int_0^H P(H^K)dH^K+H\int_H^\infty \frac{P(H^K)}{H^K}dH^K, \tag{4}$$

where the first term is the reduced remanence ($m_r=M_r/M_s$), the second one accounts for the saturated regions ($H>H^K$), and the last one is the contribution of the unsaturated regions. Equations (3) and (4) assume values of the anisotropy field up to ∞; however, this would correspond to an infinite anisotropy constant. Although this value would be unreasonable, the normalization of the distribution implies that it tends to zero as the field tends to infinity. It should be noted that in the case where there were easy axes parallel to the applied magnetic field, they would contribute equally to the remanence and have no influence on the defined distribution $P(H^K)$.

Under these assumptions, the distribution function of the perpendicular magnetic anisotropy can be obtained from the second derivative of the reduced magnetization

$$P(H^K)=-H^K\frac{d^2\langle m\rangle}{dH^2}. \tag{5}$$

In order to apply this method to the samples studied, we have to take into account the two possible orientations of the easy axes in the amorphous ribbons: due to the geometrical and dimensional characteristics of the samples, they have an easy axis directed along the ribbon axis. The other possibility of easy axis is perpendicular to the ribbon axis and is due to the stresses produced in the manufacturing of the samples. As the field will be applied along the ribbon axis, the previously described method will only provide information about the easy axes that are normal to the ribbon plane, as the other direction contributes only to the remanence.

After heat treating the ribbons in the range of the first crystallization stage, Fe,Si cubic nanocrystals appear in them. However, due to their small size ($\sim$10 nm) and to the exchange coupling across the remaining ferromagnetic amorphous matrix, the whole sample can still be represented as an ensemble of easy axes directed at right angles to the ribbon axis. The small values of the remanence to saturation magnetization ratio[10] support the assumption of small deviations of the easy axes with respect to the direction considered. If the easy axis of the anisotropy is not exactly perpendicular to the direction of the field, one can expect to find a broadening of the magnetic anisotropy distribution even for a single value of H^K and, in particular, a decrease in the symmetry of the distribution, mainly in the high field region.

When the samples are annealed in the range of the second crystallization stage, the appearance of boride-type phases causes the remanence to increase abruptly, indicating that the assumption of uniaxial easy axes with preferred orientations is no longer valid. Moreover, for samples with large hysteresis, the magnetization curve is affected by the irreversible magnetization processes, so the method loses accuracy. Therefore, the present study is limited to the first crystallization stage.

III. RESULTS

A. Hysteresis loops

The influence of the annealing temperature on the coercive field of the alloys studied is presented in Fig. 1. It can be seen that for temperatures below the crystallization onset, coercivity diminishes with annealing temperature for the three alloys. This magnetic softening in the range of temperature/time below the beginning of the isothermal nanocrystallization must have its origin in structural relaxation, as in conventional ferromagnetic alloys. It is evidenced that the structural relaxation is more effective as the silicon content is decreased, as can be seen from the lower values of the coercivity.

Hernando's model predicts a magnetic hardening when annealing at slightly higher temperatures, corresponding to the early stages of nanocrystallization. This is due to the low volume fraction of the crystallites that makes the average

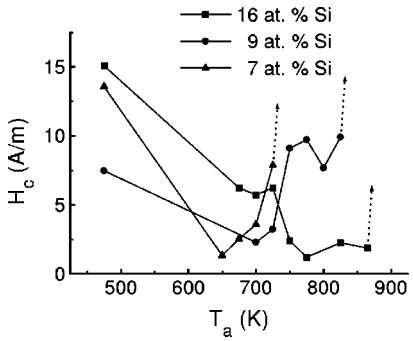

FIG. 1. Coercive field dependence with Si contents and annealing temperatures.

distance between grains much longer than the exchange correlation length between them across the amorphous matrix and prevents the magnetocrystalline anisotropy from being averaged out. The first increase of coercivity is well correlated with the onset of nanocrystallization, and is hardly detectable for the alloy containing 16 at % Si, becoming more important as the Si content is decreased. It is worth noting that the volume fractions that provoke this hardening are so small that they cannot be detected by x-ray diffraction.

When the annealing temperature and consequently the volume fraction of the crystallites is increased, Hernando's model tends to the random anisotropy model and the effective averaging of the magnetocrystalline anisotropy should cause the coercive field to decrease. This decrease is more prominent in the alloy containing 16 at % Si and its magnitude loses importance as the Si content decreases, becoming undetectable in the alloy with 7 at % Si. It should be noted that the influence of the magnetoelastic anisotropy could account for this effect, as will be pointed out later.

The final abrupt increase of coercivity is related to grain growth and the appearance of boride-type phases at the beginning of the second crystallization stage.

B. Magnetic anisotropy distribution

The evolution of magnetic anisotropy distribution with annealing temperature for the three alloys studied is presented in Figs. 2–4. Samples containing 16 at % (Fig. 2) and 9 at % Si (Fig. 3) present a more similar behavior. For both of them, when the samples are annealed at temperatures below the onset of nanocrystallization (and consequently below the increase of the coercive field), the distribution becomes narrower due to structural relaxation, which gives rise to a smoothing of the internal stresses. When the onset of nanocrystallization is reached, the distribution begins to shift to higher anisotropy fields and unfolds in various maxima. The emerging crystallites cause the internal stresses to not be the only origin of macroscopic anisotropy, but this now has a new structural component. Crystallites also develop new stresses in the sample, induced by them in the amorphous matrix. These grains cannot be exchange coupled as the exchange correlation length through the amorphous matrix is too short to cause the distant grains to interact, and therefore anisotropy cannot be averaged out. Under this condition,

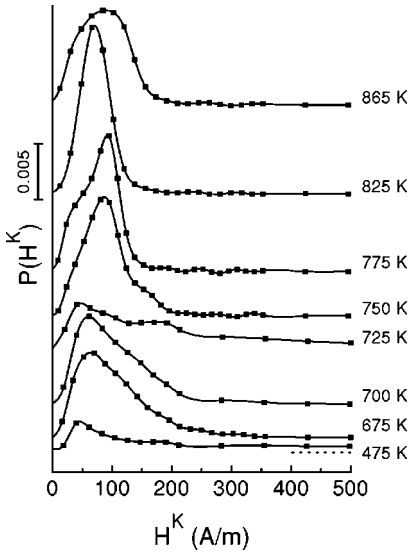

FIG. 2. Evolution of normalized magnetic anisotropy distribution with annealing temperature for the alloy containing 16 at % Si (vertical offset is provided to make the figure clearer). For the sample annealed at 475 K the dotted line is the zero-level line.

crystallites act as pinning centers for the domain walls and, consequently, magnetic hardening takes place.

Further annealing causes the crystallized volume fraction to increase and, consequently, the average distance between grains is reduced. This fact makes the distribution return to lower anisotropy fields due to the progressive averaging of the magnetocrystalline anisotropy. It should be noted, however, that the magnetic anisotropy distribution of the nanocrystallized samples is different in both cases. The sample which contains more silicon, when the optimum averaging of anisotropy is reached ($T_a = 825$ K), has a quite narrow distribution that consists of only a single maximum. On the other hand, the sample containing 9 at % Si can only reach a

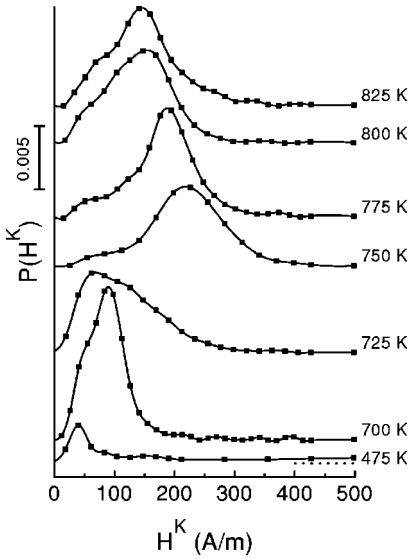

FIG. 3. Evolution of normalized magnetic anisotropy distribution with annealing temperature for the alloy containing 9 at % Si. For the sample annealed at 475 K the dotted line is the zero-level line.

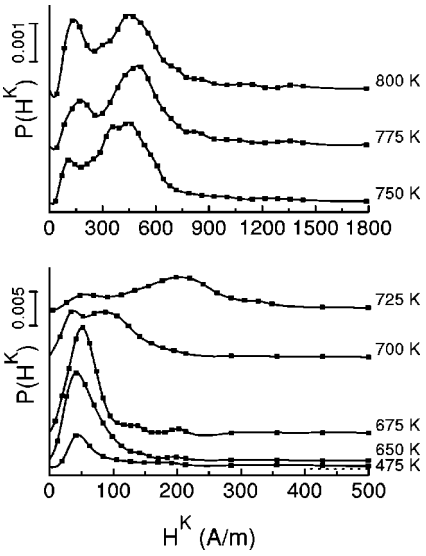

FIG. 4. Evolution of normalized magnetic anisotropy distribution with annealing temperature for the alloy containing 7 at % Si. For the sample annealed at 475 K the dotted line is the zero-level line.

distribution of magnetic anisotropy that is wider and with a mean value that is higher than that of the relaxed amorphous one.

Finally, the beginning of the second crystallization stage provokes a new broadening of the distribution, and the maxima tend to unfold again. The hardening originated by the appearance of boride-type phases causes an increase not only in the coercivity of the samples, but also in the remanence to the saturation magnetization ratio. This fact causes the method to lose accuracy, as could be seen by the loss of symmetry of the distribution when obtained from the different branches of the loop. Consequently, the second crystallization stage cannot be studied with this procedure.

The sample containing 7 at % Si (Fig. 4) has, at first sight, a different behavior. Although the stress relaxation process has the effect of narrowing the distribution, once the crystallization onset is reached, the distribution tends to grow wider and the macroscopic anisotropy does not decrease along the first crystallization stage.

IV. DISCUSSION

The first item worth noting is the continuous broadening of the magnetic anisotropy distribution for the sample containing 7 at % Si once the nanocrystallization begins. This could seem to be in contradiction with the random anisotropy model or its generalization, predicting an averaging of the magnetocrystalline anisotropy when the volume fraction increases. It should be remembered, however, that there are two contributions to the macroscopic anisotropy at this stage: the magnetocrystalline and the magnetoelastic. The former can be averaged, as predicted by the models, but the overall value of the anisotropy indicates that there is an important contribution of the latter.

Another important point is the change in depth of the coercivity minima (before and after nanocrystallization) with Si content. When the mean value of the distribution is represented versus the annealing temperature for the three samples studied (Fig. 5), it is observed that the depth of the second minimum, which is the value of $\langle H^K \rangle$ corresponding to the optimum averaging after nanocrystallization, is smaller when the Si content is decreased, to be undetectable for 7 at %. On the other hand, the behavior of the first minimum (relaxed amorphous) is the opposite: its depth is increased as the Si content is decreased. This is in agreement with the effect observed in coercivity and, consequently, the origin must be the same.

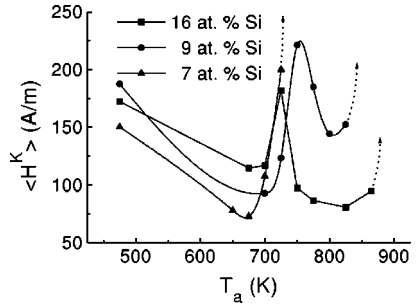

FIG. 5. Dependence of the mean anisotropy field with annealing temperature for the three alloys studied.

The plot of the magnetic anisotropy distribution for the optimally relaxed amorphous samples (Fig. 6) clearly shows that not only is the mean value increased, increasing the Si content, but the width of the distribution is also increased. This evidences a growing importance of the magnetoelastic anisotropy when the Si content is increased. If we assume that once the optimum relaxation is achieved the three samples present a similar value of the residual stresses, the presented curves can indicate an increase of λ_s of the amorphous phase, increasing the Si content. Some results reported for similar compositions ($Fe_{74.5}Nb_2Cu_1Si_xB_{22.5-x}$) support this assumption of the evolution of λ_s.[7]

As the magnetoelastic anisotropy of the nanocrystallized sample is a combination of the positive contribution of the amorphous phase and the negative one of the nanocrystals, it is logical to think that the lower the value of λ_s of the amorphous, the lower the volume fraction of crystallites that would be necessary to compensate both components. Consequently, it would be expected that the minimum value of the magnetoelastic anisotropy would be reached at lower crystallized volume fractions when the Si content of the sample

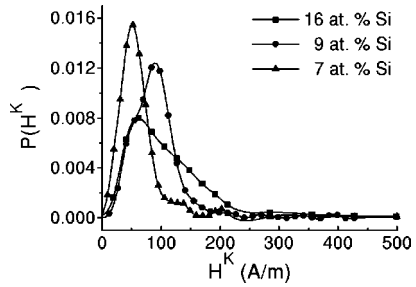

FIG. 6. Normalized magnetic anisotropy distribution of the optimally relaxed amorphous samples: (squares) 16 at % Si annealed for 1 h at 700 K; (circles) 9 at % Si annealed for 1 h at 700 K; (triangles) 7 at % Si annealed for 1 h at 675 K).

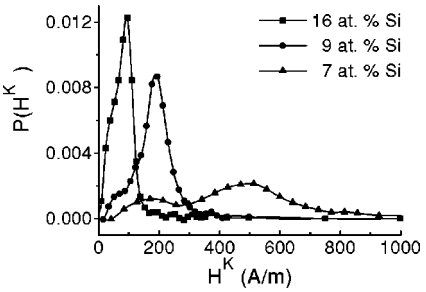

FIG. 7. Normalized magnetic anisotropy distribution of the samples annealed for 1 h at 775 K.

is decreased. This is in good agreement with the compositional dependence of the first hardening of the samples: for samples with lower Si content, the compensation of magnetoelastic anisotropy occurs at lower crystallized fractions and a further increase of the volume fraction of the crystallites provokes an increase in magnetoelastic anisotropy being so high that the averaging of the magnetocrystalline anisotropy cannot be detected. (It can only be seen annealing at 800 K for 1 h, but the distribution is so wide and flat that no claims can be made.) When the Si content is increased, the optimum value of the crystallized fraction for magnetoelastic compensation is closer to that at which the magnetocrystalline anisotropy is averaged and, consequently, the decrease of the mean value of the distribution can be seen more easily and is deeper as the Si content increases.

To support these statements, the magnetic anisotropy distribution of the samples annealed at 775 K for 1 h are presented in Fig. 7. These are the same samples whose TEM images are displayed in Fig. 8. An increasing volume fraction of the crystallites is observed when the Si content is increased. Although the sample with 7 at % Si has a lower volume fraction and a smaller mean grain size, they are not small enough to explain the huge width of the distribution. Therefore we can claim that by increasing the Si content (which provokes an increase in volume fraction), the distribution is narrowed due to the different contributions of the magnetoelastic anisotropy.

It should be noted that the value of λ_s of the amorphous phase evolves along nanocrystallization due to the changes in composition and this must be taken into account if quantitative calculus is performed. Moreover, changes in the Si content of the nanocrystals will also influence the value of their magnetostriction constant.

V. CONCLUSIONS

Throughout this work, the evolution of the magnetic anisotropy distribution of $Fe_{73.5}Si_{22.5-x}B_xCu_1Nb_3$ ($x=7,9,16$) upon heat treatment has been presented, along with coercivity data and TEM observations. The shape and mean value of the distributions are well correlated with the microstructural and magnetic data. The results obtained fall out of the capabilities of Herzer's model and have to be explained in light of the generalized random anisotropy model.

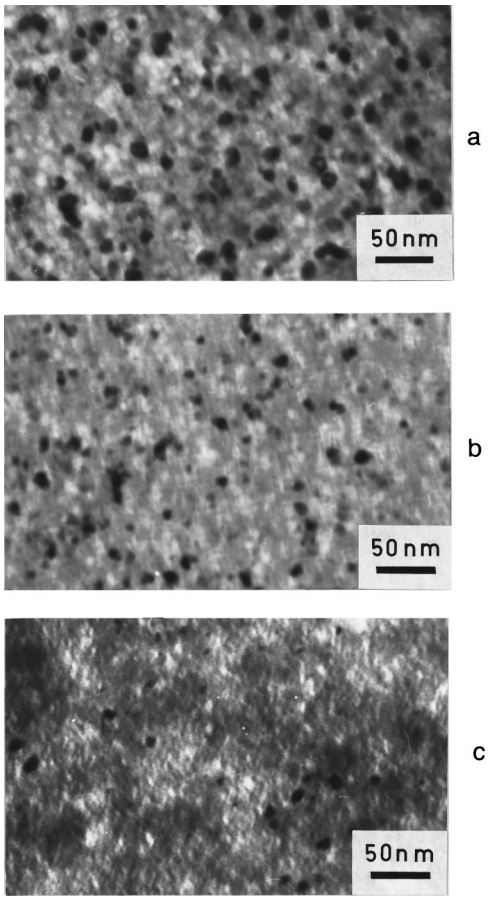

FIG. 8. TEM images of the samples annealed for 1 h at 775 K: (a) 16 at % Si; (b) 9 at % Si; (c) 7 at % Si sample.

The presented results indicate that this method is a powerful tool in the study of not only the stress relaxation process, but of the evolution of the FINEMET-type alloys along the first crystallization stage. By using the information that it provides, the behavior of the two coercivity minima (before and after nanocrystallization) with changes in the Si content can be explained: it is ascribed to the change in the compensation of magnetoelastic anisotropy due to the contributions of different signs coming from the nanocrystals and the amorphous matrix.

ACKNOWLEDGMENTS

The authors thank Dr. P. Duhaj and Dr. P. Svec (Institute of Physics of Bratislava, Slovakia) for supplying the ribbons. This work was supported by the CICYT of the Spanish Government (Project No. MAT95-0961-CO2-01) and by the PAI of the Junta de Andalucía. One of the authors, V.F., is grateful to the Fundación Cámara of the University of Sevilla for a research fellowship.

[1] Y. Yoshizawa, S. Oguma, and K. Yamauchi, J. Appl. Phys. **64**, 6044 (1988).
[2] Y. Yoshizawa and K. Yamauchi, Mater. Trans., JIM **31**, 307 (1990).
[3] F. van Bouwelen, J. Sietsma, and A. van den Beukel, J. Non-Cryst. Solids **156-158**, 567 (1993).
[4] C. F. Conde, M. Millán, and A. Conde, J. Non-Cryst. Solids **232–234** 346 (1998).
[5] V. Franco, C. F. Conde, and A. Conde, in *Non-crystalline and Nanoscale*

Materials, edited by J. Rivas and M. A. López-Quintela (World Scientific, Singapore, 1998), p. 284.
[6] M. Müller, N. Mattern, and I. Illgen, Z. Metallkd. **82**, 895 (1991).
[7] J. Zhi, K. He, L. Cheng, and Y. Fu, J. Magn. Magn. Mater. **153**, 315 (1996).
[8] C. F. Conde, V. Franco, and A. Conde, in *Rapidly Quenched and Metastable Materials*, edited by P. Duhaj, P. Mrafko, and P. Svec (Elsevier, Amsterdam, 1997), p. 254.
[9] T. Kulik and A. Hernando, J. Magn. Magn. Mater. **160**, 269 (1996).
[10] V. Franco, C. F. Conde, and A. Conde, J. Magn. Magn. Mater. **185**, 353 (1998).
[11] G. Herzer, IEEE Trans. Magn. **25**, 3327 (1989).
[12] A. Hernando, M. Vázquez, T. Kulik, and C. Prados, Phys. Rev. B **51**, 3581 (1995).
[13] V. Franco, J. Ramos-Martos, and A. Conde, Rev. Sci. Instrum. **67**, 4167 (1996).
[14] J. M. Barandiaran, M. Vázquez, A. Hernando, J. Gonzalez, and G. Rivero, IEEE Trans. Magn. **25**, 3330 (1989).